


## ARTICLE

# Metabolic analysis of the asparagine and glutamine dynamics in an industrial Chinese hamster ovary fed-batch process

Brian J. Kirsch<sup>1</sup> | Sandra V. Bennun<sup>2</sup> | Adam Mendez<sup>1</sup> | Amy S. Johnson<sup>2</sup> |  
Hongxia Wang<sup>3</sup> | Haibo Qiu<sup>3</sup> | Ning Li<sup>3</sup> | Shawn M. Lawrence<sup>2</sup> | Hanne Bak<sup>2</sup> |  
Michael J. Betenbaugh<sup>1</sup> 

<sup>1</sup>Department of Chemical and Biomolecular Engineering, Johns Hopkins University, Baltimore, Maryland, USA

<sup>2</sup>Regeneron Pharmaceuticals Inc., Preclinical Manufacturing and Process Development, Tarrytown, New York, USA

<sup>3</sup>Regeneron Pharmaceuticals Inc., Analytical Chemistry Group, Tarrytown, New York, USA

## Correspondence

Sandra V. Bennun, Regeneron Pharmaceuticals Inc., Preclinical Manufacturing and Process Development, Tarrytown, NY 10591, USA.  
Email: [sandra.bennun@regeneron.com](mailto:sandra.bennun@regeneron.com)

## Abstract

Chinese hamster ovary (CHO) cell lines are grown in cultures with varying asparagine and glutamine concentrations, but further study is needed to characterize the interplay between these amino acids. By following <sup>13</sup>C-glucose, <sup>13</sup>C-glutamine, and <sup>13</sup>C-asparagine tracers using metabolic flux analysis (MFA), CHO cell metabolism was characterized in an industrially relevant fed-batch process under glutamine supplemented and low glutamine conditions during early and late exponential growth. For both conditions MFA revealed glucose as the primary carbon source to the tricarboxylic acid (TCA) cycle followed by glutamine and asparagine as secondary sources. Early exponential phase CHO cells prefer glutamine over asparagine to support the TCA cycle under the glutamine supplemented condition, while asparagine was critical for TCA activity for the low glutamine condition. Overall TCA fluxes were similar for both conditions due to the trade-offs associated with reliance on glutamine and/or asparagine. However, glutamine supplementation increased fluxes to alanine, lactate and enrichment of glutathione, N-acetyl-glucosamine and pyrimidine-containing-molecules. The late exponential phase exhibited reduced central carbon metabolism dominated by glucose, while lactate reincorporation and aspartate uptake were preferred over glutamine and asparagine. These <sup>13</sup>C studies demonstrate that metabolic flux is process time dependent and can be modulated by varying feed composition.

## KEYWORDS

<sup>13</sup>C, asparagine, Chinese hamster ovary cells, fed-batch, glutathione, metabolic flux analysis (MFA), pyrimidine synthesis

## 1 | INTRODUCTION

The biopharmaceutical market is expected to surpass USD500 billion by 2023 (Rader & Langer, 2018). A large number of these products are generated by Chinese hamster ovary (CHO) cells, the host

organism of choice in the biopharmaceutical industry (Walsh, 2014). Efforts to understand how these cells process nutrients will increase our capacity to design medium to optimize production of recombinant proteins. One key aspect of CHO production is glutamine and asparagine metabolism, representing major carbon and nitrogen

Brian J. Kirsch and Sandra V. Bennun contributed equally to this study.

This is an open access article under the terms of the Creative Commons Attribution-NonCommercial-NoDerivs License, which permits use and distribution in any medium, provided the original work is properly cited, the use is non-commercial and no modifications or adaptations are made.

© 2021 Regeneron Pharmaceuticals, Inc. *Biotechnology and Bioengineering* published by Wiley Periodicals LLC

sources for the cell. Glutamine is a critical component, for growth, energy, redox, signaling, and pH regulation of mammalian cell metabolism (Borys et al., 1994; Dyring et al., 1994; Wahrheit et al., 2014; Xu et al., 2014). In addition to being used to synthesize protein and fuel the tricarboxylic acid (TCA) cycle, glutamine also functions as a carbon and nitrogen source for pyrimidines and their derivatives (Hayter et al., 1991; Holden et al., 1999; Mathur et al., 2017). Nucleotides from pyrimidines and purines are precursors for nucleic acid synthesis and nucleotide sugars, which are substrates for glycosylation (Evans & Guy, 2004; McAtee et al., 2014; Nyberg et al., 1999; Pels Rijcken et al., 1993).

Glutamine supplementation can alter the specific growth rate, the maximum viable cell density, titer, and the pH profile (Dean & Reddy, 2013; Wahrheit et al., 2014; Xu et al., 2014; F. Zhang et al., 2006). However, due to its high demand, glutamine is often the first amino acid to be depleted from the medium (Ahn & Antoniewicz, 2012; Chen & Harcum, 2005; Nyberg et al., 1999; Schneider et al., 1996). When fed to CHO cells, some glutamine is channeled into the TCA cycle after conversion to glutamate, which coincides with either the generation of free ammonia or excess alanine acting as a sink for ammonia (Dean & Reddy, 2013). Ammonia accumulation at higher concentrations can be detrimental for cell growth, production, and quality (Altamirano et al., 2006; Genzel et al., 2008; Gupta et al., 2017; Kurano et al., 1990). As a result, the benefits of glutamine addition to the culture can be limited. Finding the optimal level and time point for feeds can be challenging for a fed-batch process due to the balance of requirements for cell growth against cell line sensitivity to toxic quantities of ammonia.

Similar to glutamine, asparagine is of paramount importance for cellular metabolism and can sometimes fulfill a similar role to glutamine, serving as an alternative nitrogen and carbon source for the cell and can be consumed in addition to or in place of glutamine (Altamirano et al., 2006; Dean & Reddy, 2013; Duarte et al., 2014; Fomina-Yadlin et al., 2014; Genzel et al., 2008; Xu et al., 2014; J. Zhang et al., 2014; L. Zhang et al., 2016). Asparagine can also be depleted during fed-batch culture (Hansen & Emborg, 1994; Hayter et al., 1991; Kishishita et al., 2015; Xu et al., 2014). While asparagine can be important to mammalian cultures, studies have shown that glutamine, glutamate, aspartate and other metabolites can be used to compensate for asparagine-depleted conditions (Arfin et al., 1977; Seewöster & Lehmann, 1995), with limited or no effects on cell growth, antibody titer, and glycosylation of the product (Ghaffari et al., 2020). All these studies suggest that asparagine and glutamine can fulfill similar roles in metabolism, but our understanding of the interplay between these amino acids is lacking.

As glutamine and asparagine can feed the TCA cycle, their consumption rates can exceed their stoichiometric demands, therefore, a better understanding of how these amino acids are used and interplay as substrates for growth and maintenance in CHO cell cultures would be valuable. In this study a CHO cell expression platform is cultured under fed-batch mode to understand over batch time how asparagine and glutamine metabolism is modulated in glutamine supplemented and low glutamine conditions using  $^{13}\text{C}$  labeling approaches. All

conditions contained glutamine in the basal medium, with additional glutamine added in both the basal medium and feeds for the supplemented condition only. To characterize the specific contributions of asparagine, glutamine, and glucose to CHO cell metabolism during early and late exponential phase for the low glutamine and glutamine supplemented conditions, CHO cells were fed with  $^{13}\text{C}$ -glucose,  $^{13}\text{C}$ -glutamine, and  $^{13}\text{C}$ -asparagine tracers at two appropriate points during the exponential growth phase. These tracers were followed through tracer enrichment analysis and  $^{13}\text{C}$  metabolic flux analysis ( $^{13}\text{C}$  MFA). CHO cells utilized all three resources to support central carbon metabolism with characteristic patterns of utilization and distribution rates that changed from early exponential to late exponential phases. While glutamine and asparagine played key roles during the early exponential phase and were able to interchange with each other to support the TCA cycle, glucose utilization was essential as a main contributor to the TCA cycle in both the early and late exponential phases. The cells prefer glutamine over asparagine for the glutamine supplemented conditions while asparagine contributes significantly to the TCA cycle under the low glutamine condition. These amino acids also contribute to other pathways including pyrimidine, *N*-acetylglutamate (NAG), and glutathione synthesis. However, the utilization of both amino acids becomes less prominent in the late exponential growth phase as glucose, aspartate, and lactate play increasingly important roles in carbon metabolism.

## 2 | MATERIALS AND METHODS

### 2.1 | Cell culture, feeds, and tracer design

A highly engineered CHO K1-derived cell line, which does not include metabolic selective markers such as GS or DHFR, growing in suspension with a proprietary chemically defined medium was applied to produce a recombinant monoclonal antibody. The cell lines used in this fed-batch study reach peak cell densities of 30–35 million cells/ml with cell specific productivities of 23–33 pg/cell/day. Chemically defined medium and feed formulation support nutrient consumption to reach final cell titers up to 9 g/L with no statistical significance difference between both low glutamine and glutamine supplemented conditions.

Parallel cell cultures were prepared for each condition ("low glutamine" and "glutamine supplemented"), each time point (early and late exponential phase), and each of the three tracers. The tracers utilized were [U- $^{13}\text{C}$ ] asparagine, [U- $^{13}\text{C}$ ] glutamine, and a 50:50 mixture of [U- $^{13}\text{C}$ ] glucose and [1,2- $^{13}\text{C}$ ] glucose to allow for optimal resolution of pentose phosphate pathway activity (Metallo et al., 2009). After expansion in a seed train, the cells were inoculated in 250 ml shake flasks and cultured in fed-batch mode for 14 days in a humidified incubator. The basal medium contained glucose, glutamine, and asparagine. Bolus proprietary chemically defined feeds, containing the amino acids, were administered during the culture and additional glucose was fed separately each day. For each flask, a different substrate was replaced with the corresponding tracer mentioned earlier. The entirety of each of the three substrates was

replaced with tracer. The glucose, glutamine, and asparagine  $^{13}\text{C}$  tracers were fed slightly differently depending on the time point of interest (early or late exponential phase) (Figure 1a). The early exponential labeling period started with labeled basal media at inoculation time (Day 0) and continued with labeled daily glucose feeds (starting Day 1) until samples were taken on Day 2. The late exponential labeling period starts with a labeled feed on Day 4 and ends when samples were taken on Day 5. While the incubation time with tracer differs, tracer should have had more than sufficient time to perfuse through cellular metabolism in both cases. For each culture with its corresponding tracer modified in the media or feeds, sampling was performed over a brief time interval to confirm that the system reached a quasi-steady-state (Crown et al., 2016). This method involves taking triplicate samples, 3 h apart from each other, thus sampling over a 6 h period. Measurements that showed strong agreement over this period indicate isotopic steady state and are used in subsequent modeling. Measurements that differ or in a state

of change over this 6 h period are not at isotopic steady state and excluded from this study.

## 2.2 | Determination of specific consumption and production rates

The Bioprofile Flex analyzer, Bioprofile CDV and BP400 (Nova Biomedical) were used to measure glucose, lactate, ammonia, and cell number. Ultra-performance liquid chromatography (UPLC) with an AccQ•Tag Ultra C18 column was used to collect amino acid concentration data based upon absorption at 260 nm. Antibody titer was determined by high performance chromatography (HPLC) using POROS 20  $\mu\text{m}$  ProteinA ID cartridge on an Agilent HPLC column with samples detected at 280 nm absorbance.

Specific extracellular consumption and production rates of metabolites were obtained by calculating the derivatives of the

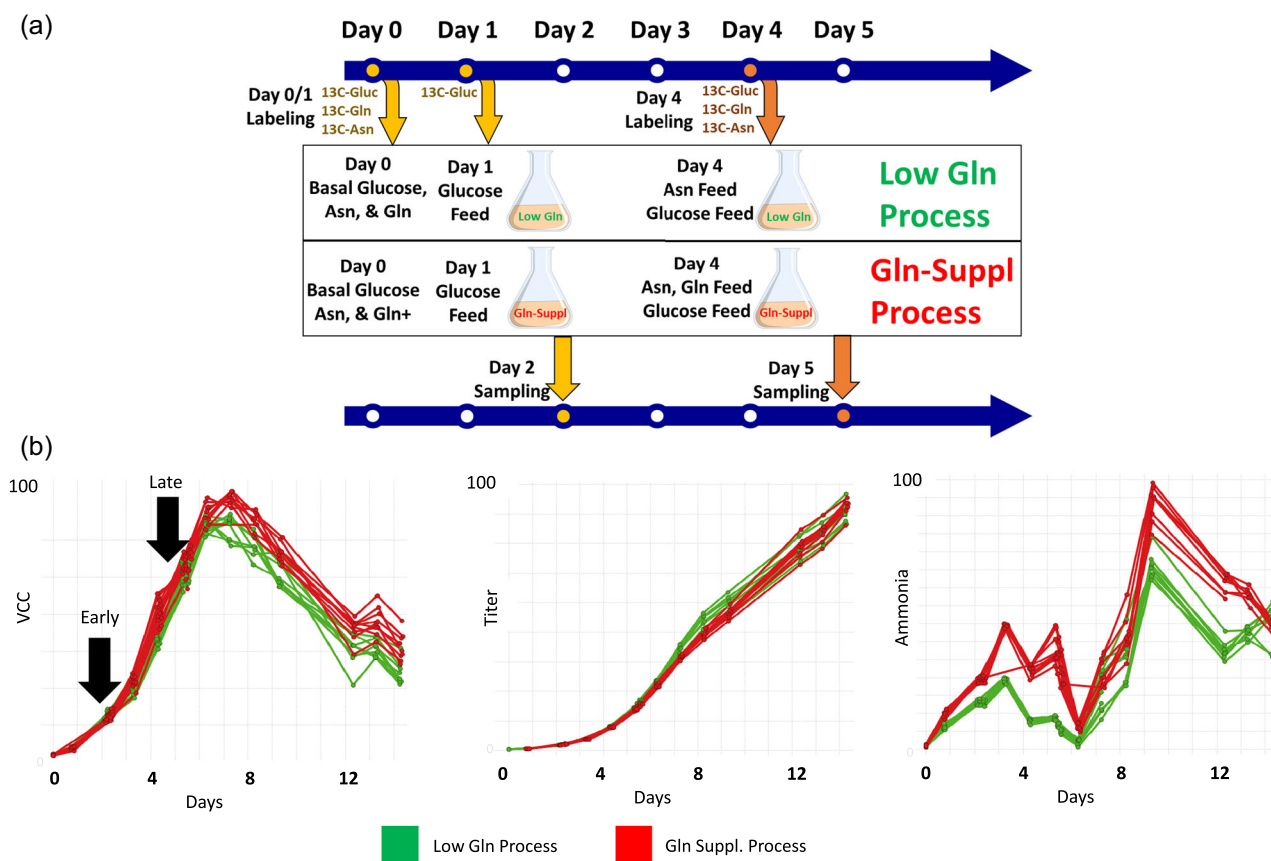


**FIGURE 1** Cell culture profiles for Chinese hamster ovary (CHO) cells in low glutamine and glutamine supplemented conditions. A process design schematic (a) for the addition of  $^{13}\text{C}$  labeled tracers (glucose, glutamine, or asparagine) for each experiment. The early exponential phase tracer additions and sampling are indicated in yellow, while the late exponential phase tracer additions and sampling are indicated in orange. The glutamine supplemented condition had additional glutamine added to the basal medium and glutamine feeds which were absent in the feeds for the low glutamine condition. All other feeds remained the same. For Day 2 samples, for tracer analysis, tracers were added to the basal medium at Day 0 and glucose feeds at Day 1. Samples were taken before feeds were added on Day 2. For Day 5 samples, tracers were added to the feeds on Day 4. (b) Normalized plots of viable cell count, antibody titer, and ammonia concentration as a function of culture time in days over the course of the CHO fed-batch process. Values were normalized to the maximum profile concentration. Multiple curves are replicates, values are given for the low glutamine (green) and the glutamine supplemented (red) conditions over the 14-day culture period

cumulative concentration profiles using a central difference method and dividing by the average cell density:

$$q_c = \frac{dC}{Xdt},$$

where  $q_c$  is the specific consumption rate of  $C$  (mmol/cell/time),  $C$  is the cumulative concentration (mmol), and  $X$  is the average cell density (cell/ml). The specific production rate of biomass was calculated using a three-parameter nonlinear equation for purposes of smoothing. Tabulated values for the fluxes calculated, normalized to the glucose input flux in low glutamine condition, are included in Table S1.

### 2.3 | Quenching, extraction, and derivatization of intracellular metabolites

Extraction and processing of gas chromatography mass spectrometry (GCMS) samples were adapted from Ahn et al. (Ahn & Antoniewicz, 2012; Ahn et al., 2016) and for liquid chromatography mass spectrometry (LCMS) were adapted from Lu et al. (2008). Samples of cells were taken 48 h after addition of the tracers for the early exponential phase and after 24 h for the late exponential phase. Approximately 10 million cells were collected from the cell culture and cold quenched.

### 2.4 | GCMS and LCMS analysis

GCMS analysis was performed on a Shimadzu GCMS-QP2010 with a Rtx-5MS (30 m × 0.25 μm × 0.25 mm i.d.) capillary column. The injection temperature was 200°C for metabolites, samples were run on splitless mode, and pressure was held at 65.2 kPa. The column flow was 1.00 ml/min and the ion source temperature was 200°C.

LCMS analysis was conducted on Acuity I-Class UPLC (Waters) coupled to a Q-Exactive™ HF mass spectrometer (Thermo Fisher Scientific). Cellular metabolites were separated on a SeQuant ZIC-pHILIC column (2.1 × 100 mm, 5 μm) (EMD Millipore). The column temperature was set at 25°C and the flow rate was 0.15 ml/min. A 25-min gradient was used for metabolites separation. Metabolites were detected in negative mode full scan analysis with resolution at 120,000.

### 2.5 | Enrichment calculation of GCMS and LCMS data

GCMS and LCMS chromatograms were analyzed and integrated for intracellular metabolites using MATLAB. Integrated peaks for the  $m+0$ ,  $m+1$ , and so forth isotopologues were converted into fractions of the total integration. Data were corrected for natural abundance using INCA (Young, 2014). Enrichments were determined

using a weighted average of the  $m+1$ ,  $m+2$ ... $m+n$  isotopologues to determine the percentage of  $^{13}\text{C}$  in the measured pool as follows:

$$\text{Enrichment} = \sum_{n=1}^N \frac{nM_n}{N},$$

where  $n$  is the number of  $^{13}\text{C}$  in a compound,  $N$  is the total number of carbons in a compound, and  $M_n$  is the percentage of the compound with  $n^{13}\text{C}$ . This results in a weighted average of all the possible isotopologues. Standard errors for enrichments were less than 1% except for lactate and malate measurements of  $^{13}\text{C}$ -glucose experiments, which were less than 2%.

### 2.6 | MFA analysis and network model of CHO metabolism

$^{13}\text{C}$ -MFA was performed using INCA (Young, 2014). INCA applies an elementary metabolite unit to estimate fluxes and minimize residuals (Antoniewicz et al., 2007; Young et al., 2008). GCMS data were used to calculate network fluxes under a steady state assumption. Standard error tabulated from the GCMS data were applied in INCA. A network of CHO carbon metabolism was adapted from previous studies (Nargund et al., 2015) as seen in Table S2. The equation for the CHO biomass and antibody was generated based on a combination of in-house analysis and distributions previously reported (Sheikh et al., 2005; Szélieová et al., 2020; Zupke et al., 1995). Fluxes and tolerances were calculated based on a 95% confidence interval of the compiled data.

## 3 | RESULTS AND DISCUSSION

### 3.1 | Glutamine supplementation upregulates glycolysis in the early exponential phase but does not prevent slowdown of glycolysis when transitioning into late exponential phase

To characterize the metabolic role of glucose, glutamine, and asparagine,  $^{13}\text{C}$ -MFA was performed on an industrially relevant CHO cell line during the early (Day 0 to Day 2) and late (Day 4 to Day 5) exponential growth phases of a fed-batch process. Two different glutamine levels, a "low glutamine" condition and a "glutamine supplemented" condition (see Section 2), were fed to a recombinant CHO cell line in a collection of shake flask fed-batch cultures (Figure 1a). Cell culture profiles of viable cell density, titer, and ammonia for the low glutamine and glutamine supplemented conditions are shown in Figure 1b. Growth rates and nutrients extracellular rates were determined throughout the fed-batch process and used in our subsequent MFA analysis (Table S2). Regardless of glutamine supplementation, the cell growth rates were relatively similar, with an early exponential growth rate of approximately  $0.05 \text{ h}^{-1}$  (Day 2) and a

late exponential growth rate of approximately  $0.016\text{ h}^{-1}$  (Day 5) for both conditions.

Glutamine supplementation increased the average peak viable cell density and ammonia levels of the culture ( $p < 0.05$ ) but did not alter the final titer significantly ( $p > 0.05$ ) (Figure 1b). For comparison purposes, the glucose uptake in the low glutamine condition during the early exponential phase was normalized on a molar basis to 100 unit/cell-day, and other fluxes are reported relative to this value (Table S1, Figure 2). For the glutamine supplemented condition in the early exponential phase, normalized glucose consumption increased to 112 unit/cell-day while lactate production increased to 73 unit/cell-day compared to 58 unit/cell-day in the low glutamine condition. Increases in lactate and ammonia (Figure 1b) were also accompanied by increases in alanine, suggesting a more active overflow metabolism with higher glucose consumption under the glutamine supplemented condition.

During the late exponential phase (Day 5), glucose consumption rate decreased to 30 unit/cell-day in both conditions (Table S1, Figure 4). The 70% decline in glucose utilization coincided with the metabolism switching to lactate uptake for both the low glutamine and glutamine supplemented conditions. Lactate consumption also differed for the two different conditions, with a lactate consumption of 4.8 unit/cell-day for the low glutamine condition and 6.7 unit/cell-day in the glutamine supplemented condition. Increases in consumption and production rates correlated with slightly increased peak cell density and enhanced ammonia production in the glutamine supplemented condition (Figure 1b). The abundance of nitrogen likely drives CHO cells to convert more pyruvate to alanine as a sink for the

intracellular nitrogen (Table S1), which has been observed previously (Chen & Harcum, 2005; McAtee Pereira et al., 2018; Ozturk et al., 1992; Schneider et al., 1996). The metabolism of glutamine and alanine are connected by the glutamine-pyruvate transaminase reaction, in which glutamine is metabolized to  $\alpha$ -ketoglutarate and the amine group produced is transferred to pyruvate, generating alanine. Through these transaminase reactions, such as that facilitated by glutamine-pyruvate and glutamate-aspartate transaminase, CHO cells can eliminate some of the excess ammonia generated, and perhaps produce a more favorable cell culture environment.

### 3.2 | Glutamine is preferred over asparagine to support the TCA cycle in the early exponential phase

$^{13}\text{C}$ -MFA was performed using GCMS data for  $^{13}\text{C}$ -glucose,  $^{13}\text{C}$ -glutamine, and  $^{13}\text{C}$ -asparagine incorporated into the media (Day 0) for both the low glutamine and the glutamine supplemented conditions. Intracellular labeling data were combined with measured extracellular flux data (Table S1) and then analyzed by the Inca MFA algorithm (Young, 2014), which minimized residuals to generate intracellular flux maps for the low glutamine and the glutamine supplemented conditions.

During the early exponential phase, approximately half of the glucose entering the cells was channeled through pyruvate into the TCA cycle for both conditions (represented as percentages in Figure 2a,b). Much of the remaining glucose consumed was converted into lactate and alanine, with higher fluxes of these

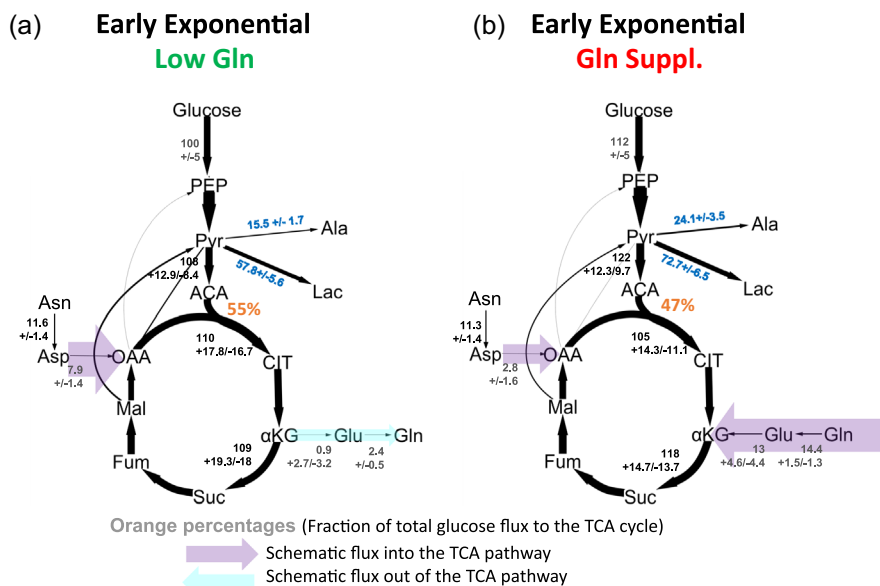


**FIGURE 2** Flux maps for early exponential phase. Early exponential phase flux maps of central carbon metabolism for the low glutamine condition (a) and glutamine supplemented condition (b). Flux values along with standard errors are normalized to glucose uptake flux of the low glutamine condition and are given in unit/cell-day with standard errors. Approximately half of the glucose-derived carbon (orange percentages) reaches the tricarboxylic acid (TCA) cycle. A detailed description of this calculation is given in the Supporting Information Methods. Blue values indicate reactions which showed statistically significant differences between conditions, while black values indicate no statistically significant differences



metabolites observed for the glutamine supplemented condition (Figure 2b). Other key secondary metabolites that enter the TCA cycle included asparagine for both conditions and glutamine in the supplemented case. While 55% and 47% of the glucose-derived carbon entered the TCA cycle (calculations detailed in the Supporting Information Methods SM.1) in the low glutamine and the glutamine supplemented conditions, respectively, asparagine and glutamine (for the glutamine supplemented condition) still provided a substantial influx into the central carbon metabolism. For the low glutamine condition, glutamine and glutamate carbon contribution to the TCA cycle was negligible while asparagine and aspartate contributed 14% of the carbon entering the TCA relative to the contribution via acetyl-CoA (ACA or AcCoA). This percentage is calculated from the ratio of fluxes entering the TCA cycle, weighted by the number carbon atoms in the source molecule. A detailed description of how this relation can be calculated is found in the Supporting Information Methods SM.2. In the glutamine supplemented condition, glutamine and glutamate provided 30% of the carbon relative to the glucose carbon contribution, while asparagine and aspartate contributed only 5% of the carbon relative to the acetyl-CoA contribution. Therefore, asparagine by way of aspartate (7.9 molar unit/cell-day, Figure 3a) was the second largest contributor of carbon to the TCA cycle for the low glutamine condition while glutamine by way of glutamate was the second largest supplement to the TCA (13 unit/cell-day, Figure 3b) in the glutamine supplemented condition. Furthermore, the asparagine/aspartate flux into the TCA cycle (2.8 unit/cell-day, Figure 3b) decreased in the glutamine supplemented condition relative to the low glutamine condition. Despite, CHO cells can use both glutamine and asparagine to support the TCA cycle along with glucose, glutamine

was clearly preferred over asparagine as indicated for the glutamine supplemented condition.

Interestingly, asparagine functions as a significant secondary resource for TCA metabolism in the low glutamine case while aspartate notably switches between excretion and consumption for the two conditions. For the low glutamine condition, aspartate was consumed (1.2 unit/cell-day Figure 3a), while in the glutamine supplemented condition aspartate was excreted (4.0 unit/cell-day, Figure 3b). Therefore, for the glutamine supplemented case, a significant fraction of the asparagine consumption leading to aspartate does not ultimately feed into the TCA as some aspartate produced left the cell or was consumed for other metabolic requirements such as biomass generation. The excretion of aspartate for these conditions may also benefit the cell by preventing further nitrogen generation. This aspartate excretion resulted in a net decrease in flux into the TCA cycle from asparagine and aspartate (Figure 2). Overall, the net changes in glutamine and asparagine fluxes into the TCA cycle in the glutamine supplemented condition (Figure 3) together with glucose input resulted in similar TCA cycle fluxes for both conditions in the early exponential phase. Interestingly, asparagine is critical in supporting growth in some cancer cells under glutamine limited conditions, which also indicates that the flux of asparagine and aspartate, in addition glutamine and glucose, can be a critical metabolic pathway for cell expansion across cell types (Pavlova et al., 2018).

### 3.3 | Aspartate is the main amino acid flux into the TCA cycle in late exponential phase

$^{13}\text{C}$ -MFA was also performed during the late exponential phase to generate intracellular flux maps for the low glutamine and glutamine supplemented conditions (Figure 4a,b). Glucose consumption was reduced to approximately 30% of that observed in early exponential phase (Figure 4a,b). Another difference from early exponential growth was that lactate served as a secondary carbon source for metabolism. Due to the greater production of lactate in the glutamine supplemented condition in the early exponential phase, more lactate was available for reuptake during the late exponential phase. Reuptake of lactate has been widely observed in previous CHO cell culture studies (Altamirano et al., 2006; Duarte et al., 2014; Freund & Croughan, 2018).

In addition, a higher fraction of glucose (and lactate)-derived carbon entered the TCA cycle for both low glutamine and glutamine supplemented conditions (>90%) during the late exponential phase (Figure 4a,b) compared to (~50%) for the early exponential phase (Figure 3a,b), perhaps in part, to the generation of fewer by-products, including serine, alanine, and glycine. Asparagine continued to provide supporting flux into TCA cycle metabolism. However, aspartate also become a key contributor of flux into the TCA cycle for both low glutamine and glutamine supplemented cases (Figure 5). In contrast, fluxes around glutamate and glutamine were minor and directed away from the TCA cycle in both conditions (Figure 5).

Interestingly, CHO cells preferentially utilized aspartate over either asparagine and glutamine in the late exponential phase for both

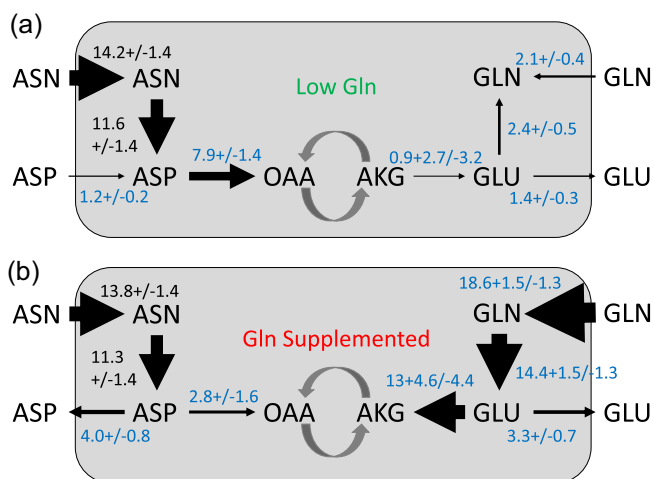


**FIGURE 3** Glutamine and asparagine metabolic flux maps during early exponential phase. Flux maps of glutamine and asparagine metabolism for the low glutamine condition (a) and glutamine supplemented condition (b). Flux values are normalized to glucose uptake flux of the low glutamine condition and are given in unit/cell-day with standard errors. Blue values indicate reactions which showed statistically significant differences between the conditions, while black values indicate no significance

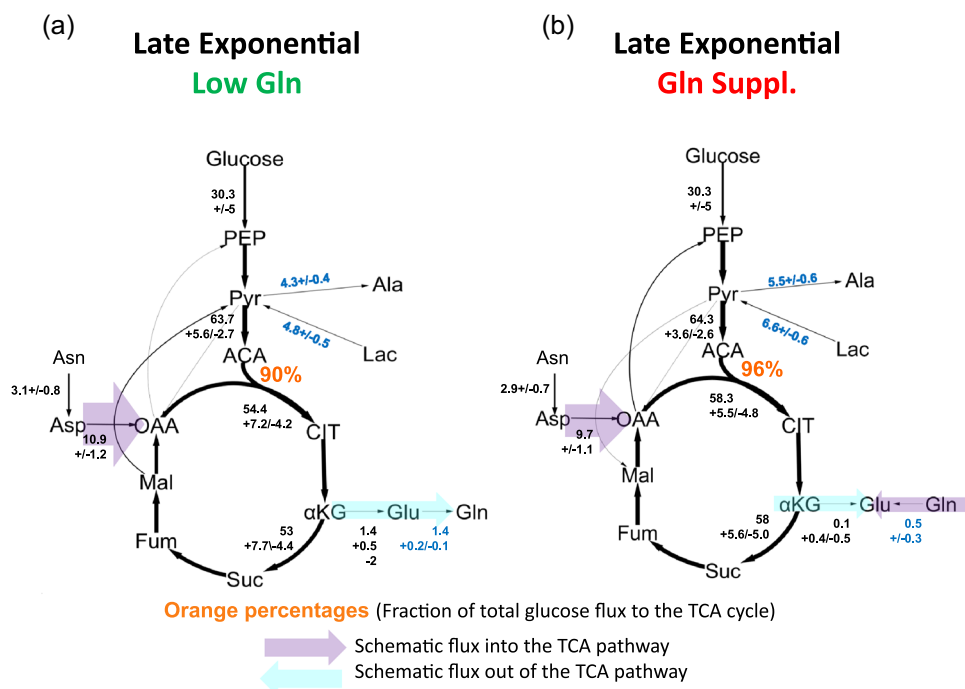


**FIGURE 4** Flux maps for late exponential phase. Late exponential phase flux maps of central carbon metabolism for the low glutamine condition (a) and glutamine supplemented condition (b). Flux values are normalized to glucose uptake flux of the low glutamine case of the early exponential phase and are given in unit/cell-day with standard errors. Glucose uptake was reduced to approximately 30% of that from the early exponential phase. More than 90% of the total glucose uptake goes into the tricarboxylic acid (TCA) (orange percentages). A detailed description of this calculation is given in the Supporting Information *Methods*. Blue values indicate reactions which showed statistically significant differences between the conditions, while black values indicate no significance

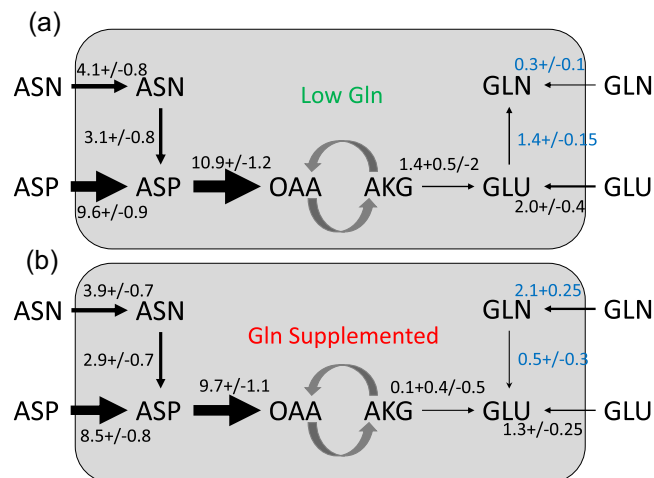


**FIGURE 5** Glutamine and asparagine metabolism flux maps for late exponential phase. Late exponential phase flux maps of glutamine and asparagine metabolism for the low glutamine condition (a) and glutamine supplemented condition (b). Flux values are normalized to the glucose uptake flux of the low glutamine case and are given in unit/cell-day with standard errors. Blue values indicate reactions which showed statistically significant differences between the conditions, while black values indicate no significance

conditions (Figure 5a,b). Asparagine fluxes were reduced by more than a factor of three during the late exponential compared to the early exponential phase for both conditions (Figures 3 and 5a,b), but the overall fractional contribution from asparagine and aspartate to the TCA was higher than during the early exponential phase. Indeed, for the low glutamine condition, aspartate and asparagine together contributed fully 40% of the carbon relative to the glucose/lactate contribution via acetyl-CoA. Also, in the glutamine supplemented condition, aspartate and asparagine contributed 33% of the carbon relative to the glucose contribution. In contrast, glutamate and glutamine drew a small amount of carbon from the TCA cycle (1.4 molar unit/cell-day) for the low glutamine condition (Figure 5a) and a negligible amount for the glutamine supplemented condition (Figure 5b).

### 3.4 | Intracellular metabolite enrichment confirms that glucose is the predominant input to the TCA in the early and late exponential phases

To further examine changes in cellular metabolism at different days and conditions, the enrichment of select metabolites derived

from the  $^{13}\text{C}$ -glucose,  $^{13}\text{C}$ -glutamine, and  $^{13}\text{C}$ -asparagine labeling experiments was estimated for the early exponential phase (Figure 6) and the late exponential phase (Figure 7).  $^{13}\text{C}$ -glutamine labeling enrichment was detected in glutamate, malate, citrate, and aspartate along with a small amount in lactate and alanine (glutamine supplemented only) during the early exponential period (Figure 6). Further, the contribution of  $^{13}\text{C}$ -glutamine in all these compounds was greater in glutamine supplemented condition.  $^{13}\text{C}$ -asparagine enrichment was noticeable in aspartate, citrate, malate, and glutamate, with a very limited level of tracer noted in other compounds (Figure 6). When additional glutamine was added, the  $^{13}\text{C}$ -asparagine enrichment in citrate, malate, and aspartate declined, indicating the preferential usage of glutamine in the TCA cycle and its intermediates and by-products.

During the late exponential phase,  $^{13}\text{C}$ -glucose enrichment remained predominant while the enrichment from  $^{13}\text{C}$ -glutamine and  $^{13}\text{C}$ -asparagine declined for many metabolites in both conditions (Figure 7). Lactate, pyruvate, alanine, glycine, and serine were dominated by  $^{13}\text{C}$ -glucose enrichment over  $^{13}\text{C}$ -glutamine and  $^{13}\text{C}$ -asparagine. Glucose also contributed a substantial percentage to citrate, malate, and glutamate, but a smaller percentage of aspartate. This is consistent with the flux analysis which indicates that unlabeled aspartate represents a principal contributor to the TCA after glucose in the late exponential phase.

Limited amounts of  $^{13}\text{C}$ -asparagine were detected in aspartate, citrate, glutamate, and lactate (in the glutamine supplemented condition). Its reduction relative to the early exponential phase is likely due to the increased uptake of aspartate in both the low glutamine and glutamine supplemented conditions (Figure 5a,b).  $^{13}\text{C}$ -glutamine

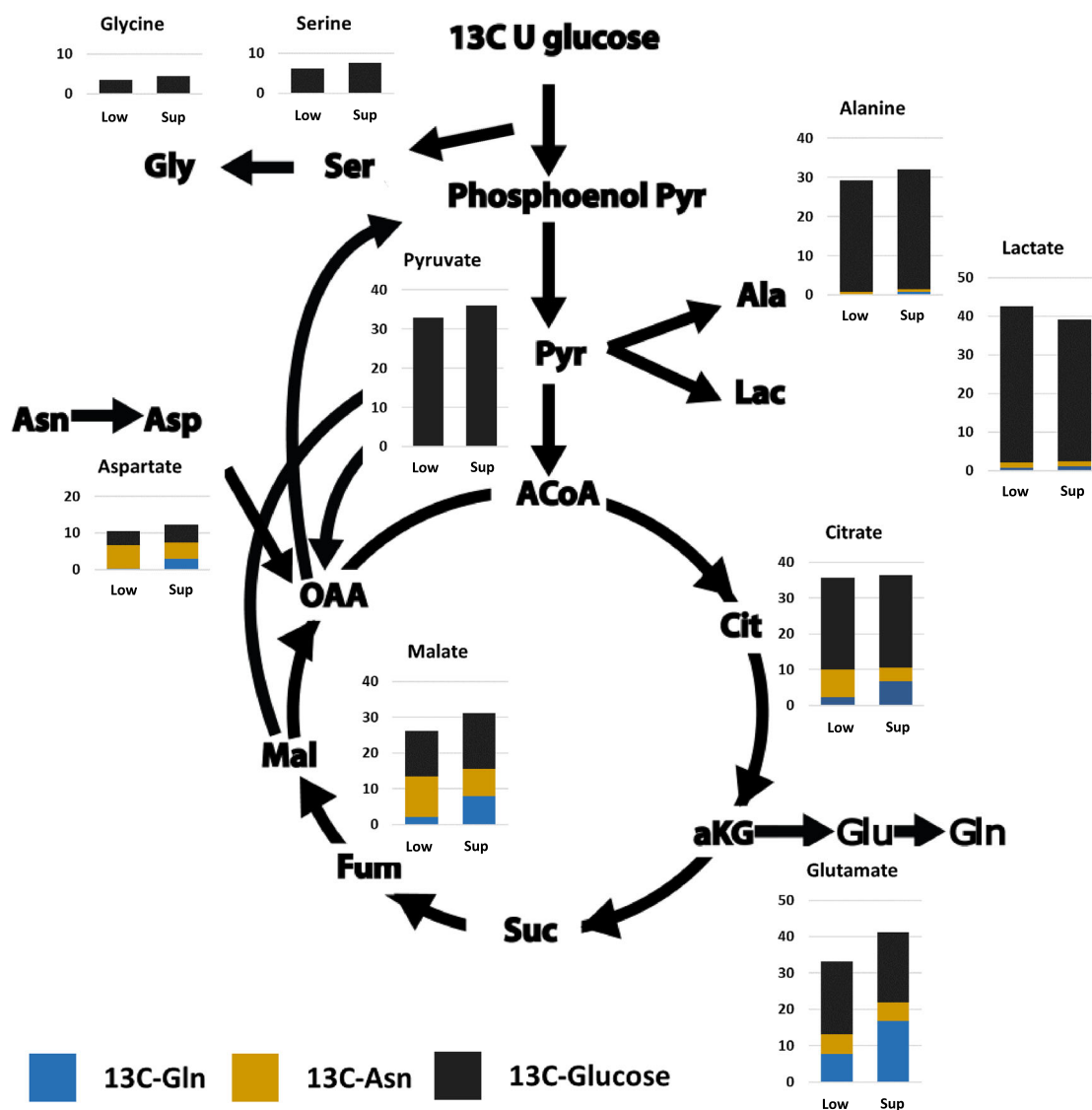


**FIGURE 6** Early exponential phase intracellular metabolite enrichment. Enrichment in select free metabolites from  $^{13}\text{C}$ -glucose (black),  $^{13}\text{C}$ -glutamine (blue), and  $^{13}\text{C}$ -asparagine (yellow) for the early exponential phase is shown in the inset graphs. Enrichments are shown for the low glutamine (Low) and glutamine supplemented (Sup) conditions



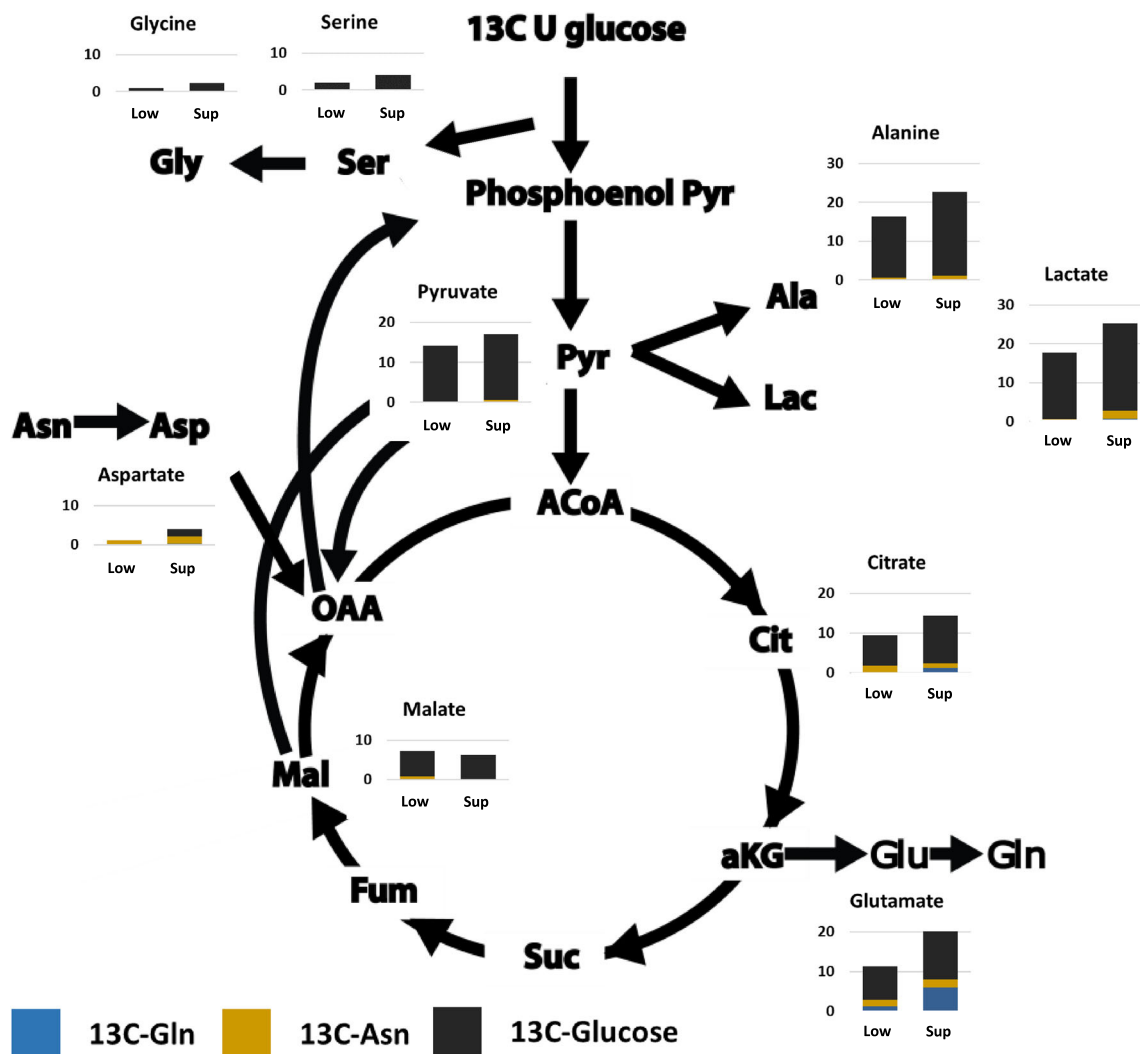


**FIGURE 7** Late exponential phase intracellular metabolite enrichment. Enrichment in select free metabolites from  $^{13}\text{C}$ -glucose (black),  $^{13}\text{C}$ -glutamine (blue), and  $^{13}\text{C}$ -asparagine (yellow) experiments for the late exponential phase is shown in the inset graphs. Enrichments are shown for the low glutamine (Low) and glutamine supplemented (Sup) conditions

noticeably labeled glutamate but principally in the glutamine supplemented conditions. Only trace amounts of  $^{13}\text{C}$ -glutamine were detected in citrate and lactate. The enrichment results support the predominance of  $^{13}\text{C}$ -glucose tracer incorporation in all the measured metabolites, and the major role that glucose plays in supporting the TCA cycle during both phases, especially during the late exponential phase.

### 3.5 | Glutamine supplementation increases intracellular enrichment of nitrogen containing molecules in the early exponential phase

The role that glutamine and asparagine play in other metabolic pathways was also examined using LCMS during the early exponential phase when glutamine and asparagine incorporation into other metabolites was elevated. Significant  $^{13}\text{C}$ -glutamine and

$^{13}\text{C}$ -asparagine labeling of metabolites was detected for pyrimidines, glutathione, and NAG pathways in both low glutamine and glutamine supplemented conditions (Figure 8). The pyrimidine synthesis pathway utilizes the initial precursors carbamoyl phosphate and aspartate to begin synthesis of other subsequent precursors and products (Figure 8a). Carbon enters the pyrimidine synthesis pathway through aspartate (Mathur et al., 2017). Therefore, glutamine and asparagine must first be converted to aspartate. In addition, the initial step of this pathway is glutamine dependent, due to the key role of glutamine as a nitrogen provider. Although glutamine does not contribute carbon directly, perhaps its increased availability may help to drive pathway activity in glutamine supplemented cultures by contributing some aspartate generation in the supplemented condition (Figure 6). Noticeable  $^{13}\text{C}$  enrichment from  $^{13}\text{C}$ -asparagine and  $^{13}\text{C}$ -glutamine was detected for *N*-carbamoyl-aspartate, UMP, UTP, deoxyuridine, and dTTP, all of which showed increased enrichment from  $^{13}\text{C}$ -glutamine for the glutamine supplemented condition (Figure 8b).

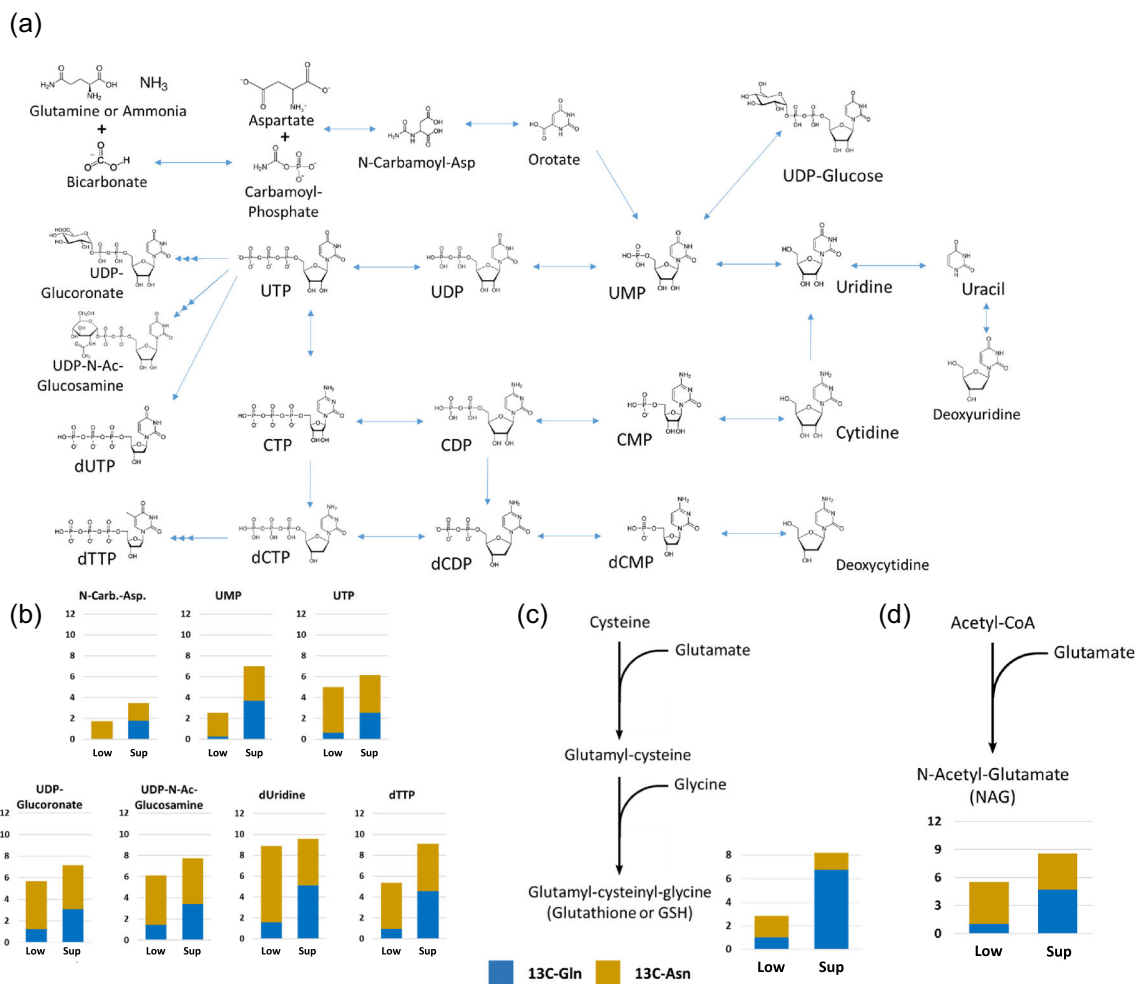


**FIGURE 8** Early exponential phase enrichment of intracellular nucleotides, nucleotide-derivatives, and glutathione. Reaction network for pyrimidine synthesis originating from aspartate and glutamine (a). Reversible reactions and direction reactions are specified based on KEGG pathways. Enrichments for the early exponential phase are shown for the low glutamine (Low) and glutamine supplemented (Sup) conditions. Experimental <sup>13</sup>C-glutamine (blue) and <sup>13</sup>C-asparagine (yellow) data are shown for in select free nucleotides and nucleotide derivatives (b). Glutathione is synthesized from the amino acids cysteine, glycine, and glutamate (c). N-acetyl glutamate (NAG) is synthesized from acetyl-CoA and glutamate from (d)

We also observed enrichment in nucleotide sugars including UDP-glucuronate and UDP-GlcNAc for the glutamine supplemented cultures. This role of glutamine for production of UDP sugars has been noted previously for mammalian cell lines (Burleigh et al., 2011; Mathur et al., 2017; Taschwer et al., 2012), and UDP-GlcNAc levels can have a significant impact on glycosylation of IgG and other cellular glycoproteins (Burleigh et al., 2011; Fan et al., 2012; Hills et al., 2001). Enrichment from <sup>13</sup>C-asparagine exhibited some fluctuations but remained consistent for most compounds in both conditions.

Glutathione is an antioxidant tripeptide synthesized from glycine, cysteine, and glutamate. As glutamine was supplemented, the fraction of enriched glutathione increased threefold (Figure 8c). Since the enrichment from <sup>13</sup>C-asparagine slightly decreased, most of this increase came from the <sup>13</sup>C-glutamine. Cultures in which glutamine is elevated have been known to exhibit an increase in the levels of glutathione (Amores-Sánchez & Medina, 1999; Hong et al., 1992;

Sies, 1999). Glutathione itself has been found to be an antioxidant that controls reactive oxygen species and inhibits apoptosis (Al-Rubeai & Singh, 1998; Amores-Sánchez & Medina, 1999; Franco & Cidowski, 2009; Sies, 1999) as well as regulating disulfide bonds in proteins (Chakravarthi & Bulleid, 2004; Chiosa et al., 1965; Sies, 1999). Providing glutamine to cultures may thus provide beneficial impacts well beyond TCA cycle metabolism such as facilitating the generation of glutathione and other metabolites that can provide resistance against apoptosis and alter the protein folding and redox environment (Orellana et al., 2015). This may help explain, at least in part, the slight increase in cell densities observed in the VCC measurements of the glutamine supplemented condition.

In addition, the metabolite, NAG, derived from glutamine as shown in Figure 8d was enriched from <sup>13</sup>C-asparagine with a significant boost in enrichment following <sup>13</sup>C-glutamine supplementation (Figure 8d). NAG serves as an activator of the initial steps of the urea cycle, which are identical to those in pyrimidine synthesis

(Anderson, 1981; Holden et al., 1999; Levenberg, 1962; Makoff & Radford, 1976) although NAG is not known to promote the pyrimidine pathway. Increased expression of urea cycle enzymes in the CHO cells is known to result in reduced accumulation of ammonium ions in the culture medium (Chung et al., 2003). Overall, glutathione and pyrimidine pathway enrichment along with NAG increases under glutamine supplemented medium may provide supplemental benefits to cell growth and robustness beyond the direct effects of glutamine's impact on the TCA cycle.

## 4 | CONCLUSIONS

<sup>13</sup>C MFA was used to examine the distribution of glucose, glutamine, and asparagine at different points of the exponential growth phase for a low glutamine condition with glutamine in the basal medium only compared to a condition with glutamine supplementation in the feeds in addition to the basal medium for an industrially relevant fed-batch process. While glucose is the primary carbon source into the TCA cycle during the exponential phase, glucose uptake rates and fluxes decrease from the early to the late exponential phase. However, the percent contribution of carbon from glucose to the TCA cycle increases at later times. In contrast, glutamine and asparagine are the preferred secondary carbon sources during the early exponential growth phase. Glutamine was favored over asparagine in the glutamine supplemented condition, while asparagine was more important for the low glutamine condition. In addition, for the glutamine supplemented condition, lactate, alanine, and ammonia fluxes were elevated during the early exponential phase. This suggests a link between glutamine consumption and glycolysis activity, which is reminiscent of the metabolic rewiring in cancer cells whereby increased lactate production from glucose, known as the "Warburg effect," often coincides with "glutamine addiction" (Alberghina & Gaglio, 2014; DeBerardinis et al., 2008; Le et al., 2012; Warburg, 1956). Flux data indicate a dynamic change in the glucose to amino acid ratio channeled into the TCA as the culture progresses from early to late exponential phase with glutamine input into TCA cycle activity becoming negligible and asparagine uptake dropping threefold regardless of glutamine supplementation. Interestingly, aspartate was preferentially utilized during the late exponential phase for both the low glutamine and glutamine supplemented cultures perhaps due to either increased excretion during the early exponential phase or its potential preference as a substrate for the slower-growing late exponential cells. This suggests the importance of consistent aspartate supplementation in the late exponential phase when glutamine is being produced and asparagine is highly consumed. We recognize, however, that there is a considerable diversity between CHO cell lines, and thus the relative importance of the various substrates may vary across cell lines.

While TCA fluxes appeared comparable for glutamine supplemented and low glutamine conditions, enrichment data and <sup>13</sup>C MFA indicates that the glutamine supplemented condition leads to greater lactate production in the early exponential phase, resulting in a larger

lactate reservoir. Furthermore, complementary LC analysis during the early exponential phase indicated notable enrichment of *N*-acetylglucosamine, glutathione, and various pyrimidines, leading to enrichment of nucleotides and nucleotide sugars such as UDP-GlcNAc in glutamine supplemented conditions. While glutamine supplementation is not essential for sufficient cell growth, its presence may impact cellular energetics via TCA cycle intermediates and glycosylation via sugar nucleotides such as UDP-GlcNAc and other pyrimidine pathway derivatives. Enrichment of metabolites such as glutathione can impact other pathways including the inhibition of reactive oxygen species which can in turn limit the activation of apoptosis (Mailloux et al., 2013; Redza-Dutordoir & Averill-Bates, 2016). Therefore, supplementing cultures with the proper glutamine concentrations that balance the benefits of glutamine availability versus by-product accumulation such as lactate and ammonia may ultimately be beneficial for cell cultures.

## ACKNOWLEDGMENTS

The authors would like to thank Dr. Phil Mortimer for his support with GCMS and all the PMPD analytics group for amino acid and monoclonal antibody titer measurements, in special to John Reeves and Rebecca Lawlor.

## DATA AVAILABILITY STATEMENT

The data that support the findings of this study are available from the corresponding author upon reasonable request.

## ORCID

Michael J. Betenbaugh  <http://orcid.org/0000-0002-6336-4659>

## REFERENCES

- Ahn, W. S., & Antoniewicz, M. R. (2012). Towards dynamic metabolic flux analysis in CHO cell cultures. *Biotechnology Journal*, 7, 61–74.
- Ahn, W. S., Crown, S. B., & Antoniewicz, M. R. (2016). Evidence for transketolase-like TKTL1 flux in CHO cells based on parallel labeling experiments and 13 C-metabolic flux analysis. *Metabolic Engineering*, 37, 72–78.
- Alberghina, L., & Gaglio, D. (2014). Redox control of glutamine utilization in cancer. *Cell Death & Disease*, 5, e1561.
- Al-Rubeai, M., & Singh, R. P. (1998). Apoptosis in cell culture. *Current Opinion in Biotechnology*, 9, 152–156.
- Altamirano, C., Illanes, A., Becerra, S., Cairó, J. J., & Gòdia, F. (2006). Considerations on the lactate consumption by CHO cells in the presence of galactose. *Journal of Biotechnology*, 125, 547–556.
- Amores-Sánchez, M. I., & Medina, M. Á. (1999). Glutamine, as a precursor of glutathione, and oxidative stress. *Molecular Genetics and Metabolism*, 67, 100–105.
- Anderson, P. M. (1981). Purification and properties of the glutamine- and *N*-acetyl-L-glutamate-dependent carbamoyl phosphate synthetase from liver of *Squalus acanthias*. *Journal of Biological Chemistry*, 256, 12228–12238.
- Antoniewicz, M. R., Kelleher, J. K., & Stephanopoulos, G. (2007). Elementary metabolite units (EMU): A novel framework for modeling isotopic distributions. *Metabolic Engineering*, 9, 68–86.
- Arfin, S. M., Simpson, D. R., Chiang, C. S., Andrulis, I. L., & Hatfield, G. W. (1977). A role for asparaginyl-tRNA in the regulation of asparagine synthetase in a mammalian cell line. *Proceedings of the National Academy of Sciences*, 74, 2367–2369.

- Borys, M. C., Linzer, D. I. H., & Papoutsakis, E. T. (1994). Ammonia affects the glycosylation patterns of recombinant mouse placental lactogen-I by Chinese hamster ovary cells in a pH-dependent manner. *Biotechnology and Bioengineering*, 43, 505–514.
- Burleigh, S. C., van de Laar, T., Stroop, C. J., van Grunsven, W. M., O'Donoghue, N., Rudd, P. M., & Davey, G. P. (2011). Synergizing metabolic flux analysis and nucleotide sugar metabolism to understand the control of glycosylation of recombinant protein in CHO cells. *BMC Biotechnology*, 11, 95.
- Chakravarthi, S., & Bulleid, N. J. (2004). Glutathione is required to regulate the formation of native disulfide bonds within proteins entering the secretory pathway. *Journal of Biological Chemistry*, 279, 39872–39879.
- Chen, P., & Harcum, S. W. (2005). Effects of amino acid additions on ammonium stressed CHO cells. *Journal of Biotechnology*, 117, 277–186.
- Chiosa, L., Niculescu, V., Bonciocat, C., & Stancu, C. (1965). The protective action of N-acetyl and N-carbamyl derivatives of glutamic and aspartic acids against ammonia intoxication. *Biochemical Pharmacology*, 14, 1635–1643.
- Chung, M.-I., Lim, M.-H., Lee, Y.-J., Kim, I.-H., Kim, I.-Y., Kim, J.-H., Chang, K.-H., & Kim, H.-J. (2003). Reduction of ammonia accumulation and improvement of cell viability by expression of urea cycle enzymes in Chinese hamster ovary cells. *Journal of Microbiology and Biotechnology*, 13, 217–224.
- Crown, S. B., Long, C. P., & Antoniewicz, M. R. (2016). Optimal tracers for parallel labeling experiments and 13C metabolic flux analysis: A new precision and synergy scoring system. *Metabolic Engineering*, 38, 10–18.
- Dean, J., & Reddy, P. (2013). Metabolic analysis of antibody producing CHO cells in fed-batch production. *Biotechnology and Bioengineering*, 110, 1735–1747.
- DeBerardinis, R. J., Lum, J. J., Hatzivassiliou, G., & Thompson, C. B. (2008). The biology of cancer: Metabolic reprogramming fuels cell growth and proliferation. *Cell Metabolism*, 7, 11–20.
- Duarte, T. M., Carinhas, N., Barreiro, L. C., Carrondo, M. J. T., Alves, P. M., & Teixeira, A. P. (2014). Metabolic responses of CHO cells to limitation of key amino acids. *Biotechnology and Bioengineering*, 111, 2095–2106.
- Dyring, C., Hansen, H. A., & Emborg, C. (1994). Observations on the influence of glutamine, asparagine and peptone on growth and t-PA production of Chinese hamster ovary (CHO) cells. *Cytotechnology*, 16, 37–42.
- Evans, D. R., & Guy, H. I. (2004). Mammalian pyrimidine biosynthesis: Fresh insights into an ancient pathway. *Journal of Biological Chemistry*, 279, 33035–33038.
- Fan, L., Kadura, I., Krebs, L. E., Hatfield, C. C., Shaw, M. M., & Frye, C. C. (2012). Improving the efficiency of CHO cell line generation using glutamine synthetase gene knockout cells. *Biotechnology and Bioengineering*, 109, 1009–1015.
- Fomina-Yadlin, D., Gosink, J. J., McCoy, R., Follstad, B., Morris, A., Russell, C. B., & McGrew, J. T. (2014). Cellular responses to individual amino-acid depletion in antibody-expressing and parental CHO cell lines. *Biotechnology and Bioengineering*, 111, 965–979.
- Franco, R., & Cidlowski, J. A. (2009). Apoptosis and glutathione: Beyond an antioxidant. *Cell Death & Differentiation*, 16, 1303–1314.
- Freund, N., & Croughan, M. (2018). A simple method to reduce both lactic acid and ammonium production in industrial animal cell culture. *International Journal of Molecular Sciences*, 19, 385.
- Genzel, Y., Ritter, J. B., König, S., Alt, R., & Reichl, U. (2008). Substitution of glutamine by pyruvate to reduce ammonia formation and growth inhibition of mammalian cells. *Biotechnology Progress*, 21, 58–69.
- Ghaffari, N., Jardon, M. A., Krahn, N., Butler, M., Kennard, M., Turner, R. F. B., Gopaluni, B., & Piret, J. M. (2020). Effects of cysteine, asparagine, or glutamine limitations in Chinese hamster ovary cell batch and fed-batch cultures. *Biotechnology Progress*, 36, e2946.
- Gupta, S. K., Srivastava, S. K., Sharma, A., Nalage, V. H. H., Salvi, D., Kushwaha, H., Chitnis, N. B., & Shukla, P. (2017). Metabolic engineering of CHO cells for the development of a robust protein production platform. *PLoS One*, 12, e0181455.
- Hansen, H. A., & Emborg, C. (1994). Influence of ammonium on growth, metabolism, and productivity of a continuous suspension Chinese hamster ovary cell culture. *Biotechnology Progress*, 10, 121–124.
- Hayter, P. M., Curling, E. M. A., Baines, A. J., Jenkins, N., Salmon, I., Strange, P. G., & Bull, A. T. (1991). Chinese hamster ovary cell growth and interferon production kinetics in stirred batch culture. *Applied Microbiology and Biotechnology*, 34, 559–564.
- Hills, A. E., Patel, A., Boyd, P., & James, D. C. (2001). Metabolic control of recombinant monoclonal antibody N-glycosylation in GS-NSO cells. *Biotechnology and Bioengineering*, 75, 239–251.
- Holden, H. M., Thoden, J. B., & Raushel, F. M. (1999). Carbamoyl phosphate synthetase: An amazing biochemical odyssey from substrate to product. *Cellular and Molecular Life Sciences (CMLS)*, 56, 507–522.
- Hong, R. W., Rounds, J. D., Helton, W. S., Robinson, M. K., & Wilmore, D. W. (1992). Glutamine preserves liver glutathione after lethal hepatic injury. *Annals of Surgery*, 215, 114–119.
- Kishishita, S., Katayama, S., Kodaira, K., Takagi, Y., Matsuda, H., Okamoto, H., Takuma, S., Hirashima, C., & Aoyagi, H. (2015). Optimization of chemically defined feed media for monoclonal antibody production in Chinese hamster ovary cells. *Journal of Bioscience and Bioengineering*, 120, 78–84.
- Kurano, N., Leist, C., Messi, F., Kurano, S., & Fiechter, A. (1990). Growth behavior of Chinese hamster ovary cells in a compact loop bioreactor. 2. Effects of medium components and waste products. *Journal of Biotechnology*, 15, 113–128.
- Le, A., Lane, A. N., Hamaker, M., Bose, S., Gouw, A., Barbi, J., Tsukamoto, T., Rojas, C. J., Slusher, B. S., Zhang, H., Zimmerman, L. J., Liebler, D. C., Slebos, R. J. C., Lorkiewicz, P. K., Higashi, R. M., Fan, T. W. M., & Dang, C. V. (2012). Glucose-independent glutamine metabolism via TCA cycling for proliferation and survival in B cells. *Cell Metabolism*, 15, 110–121.
- Levenberg, B. (1962). Role of L-glutamine as donor of carbamyl nitrogen for the enzymatic synthesis of citrulline in *Agaricus bisporus*. *Journal of Biological Chemistry*, 237, 2590–2598.
- Lu, W., Bennett, B. D., & Rabinowitz, J. D. (2008). Analytical strategies for LC-MS-based targeted metabolomics. *Journal of Chromatography B*, 871, 236–242.
- Mailloux, R. J., McBride, S. L., & Harper, M.-E. (2013). Unearthing the secrets of mitochondrial ROS and glutathione in bioenergetics. *Trends in Biochemical Sciences*, 38, 592–602.
- Makoff, A. J., & Radford, A. (1976). Glutamine utilization in both the arginine-specific and pyrimidine-specific carbamoyl phosphate synthase enzymes of *Neurospora crassa*. *Molecular and General Genetics MGG*, 149, 175–178.
- Mathur, D., Stratikopoulos, E., Ozturk, S., Steinbach, N., Pegno, S., Schoenfeld, S., Yong, R., Murty, V., Asara, J. M., Cantley, L. C., & Parsons, R. (2017). PTEN regulates glutamine flux to pyrimidine synthesis and sensitivity to dihydroorotate dehydrogenase inhibition. *Cancer Discovery*, 7, 380–390.
- McAtee, A. G., Templeton, N., & Young, J. D. (2014). Role of Chinese hamster ovary central carbon metabolism in controlling the quality of secreted biotherapeutic proteins. *Pharmaceutical Bioprocessing*, 2, 63–74.
- McAtee Pereira, A. G., Walther, J. L., Hollenbach, M., & Young, J. D. (2018). <sup>13</sup>C flux analysis reveals that rebalancing medium amino acid composition can reduce ammonia production while preserving

- central carbon metabolism of CHO cell cultures. *Biotechnology Journal*, 13, e1700518.
- Metallo, C. M., Walther, J. L., & Stephanopoulos, G. (2009). Evaluation of  $^{13}\text{C}$  isotopic tracers for metabolic flux analysis in mammalian cells. *Journal of Biotechnology*, 144, 167–174.
- Nargund, S., Qiu, J., & Goudar, C. T. (2015). Elucidating the role of copper in CHO cell energy metabolism using  $^{13}\text{C}$  metabolic flux analysis. *Biotechnology Progress*, 31, 1179–1186.
- Nyberg, G. B., Balcarcel, R. R., Follstad, B. D., Stephanopoulos, G., & Wang, D. I. C. (1999). Metabolism of peptide amino acids by Chinese hamster ovary cells grown in a complex medium. *Biotechnology and Bioengineering*, 62, 324–335.
- Orellana, C. A., Marcellin, E., Schulz, B. L., Nouwens, A. S., Gray, P. P., & Nielsen, L. K. (2015). High-antibody-producing chinese hamster ovary cells up-regulate intracellular protein transport and glutathione synthesis. *Journal of Proteome Research*, 14, 609–618.
- Ozturk, S. S., Riley, M. R., & Palsson, B. O. (1992). Effects of ammonia and lactate on hybridoma growth, metabolism, and antibody production. *Biotechnology and Bioengineering*, 39, 418–431.
- Pavlova, N. N., Hui, S., Ghergurovich, J. M., Fan, J., Intlekofer, A. M., White, R. M., Rabinowitz, J. D., Thompson, C. B., & Zhang, J. (2018). As extracellular glutamine levels decline, asparagine becomes an essential amino acid. *Cell Metabolism*, 27, 428–438.e5.
- Pels Rijcken, W. R., Overdijk, B., van den Eijnden, D. H., & Ferwerda, W. (1993). Pyrimidine nucleotide metabolism in rat hepatocytes: evidence for compartmentation of nucleotide pools. *Biochemical Journal*, 293, 207–213.
- Rader, R. A., & Langer, E. S. (2018). *Biopharma manufacturing markets*. [https://www.contractpharma.com/issues/2018-05-01/view\\_features/biopharma-manufacturing-markets/](https://www.contractpharma.com/issues/2018-05-01/view_features/biopharma-manufacturing-markets/)
- Redza-Dutordoir, M., & Averill-Bates, D. A. (2016). Activation of apoptosis signalling pathways by reactive oxygen species. *Biochimica et Biophysica Acta (BBA)—Molecular Cell Research*, 1863, 2977–2992.
- Schneider, M., M., IanW, & von Stockar U. (1996). The importance of ammonia in mammalian cell culture. *Journal of Biotechnology*, 46, 161–185.
- Seewöster, T., & Lehmann, J. (1995). Influence of targeted asparagine starvation on extra- and intracellular amino acid pools of cultivated Chinese hamster ovary cells. *Applied Microbiology and Biotechnology*, 44, 344–350.
- Sheikh, K., Förster, J., & Nielsen, L. K. (2005). Modeling hybridoma cell metabolism using a generic genome-scale metabolic model of *Mus musculus*. *Biotechnology Progress*, 21, 112–121.
- Sies, H. (1999). Glutathione and its role in cellular functions. *Free Radical Biology and Medicine*, 27, 916–921.
- Széliová, D., Ruckerbauer, D. E., Galleguillos, S. N., Petersen, L. B., Natter, K., Hanscho, M., Troyer, C., Causon, T., Schoeny, H., Christensen, H. B., Lee, D.-Y., Lewis, N. E., Koellensperger, G., Hann, S., Nielsen, L. K., Borth, N., & Zanghellini, J. (2020). What CHO is made of: Variations in the biomass composition of Chinese hamster ovary cell lines. *Metabolic Engineering*, 61, 288–300.
- Taschwer, M., Hackl, M., Hernández Bort, J. A., Leitner, C., Kumar, N., Puc, U., Grass, J., Papst, M., Kunert, R., Altmann, F., & Borth, N. (2012). Growth, productivity and protein glycosylation in a CHO EpoFc producer cell line adapted to glutamine-free growth. *Journal of Biotechnology*, 157, 295–303.
- Wahrheit, J., Nicolae, A., & Heinzle, E. (2014). Dynamics of growth and metabolism controlled by glutamine availability in Chinese hamster ovary cells. *Applied Microbiology and Biotechnology*, 98, 1771–1783.
- Walsh, G. (2014). Biopharmaceutical benchmarks 2014. *Nature Biotechnology*, 32, 992–1000.
- Warburg, O. (1956). On the origin of cancer cells. *Science*, 123, 309–314.
- Xu, P., Dai, X.-P., Graf, E., Martel, R., & Russell, R. (2014). Effects of glutamine and asparagine on recombinant antibody production using CHO-GS cell lines. *Biotechnology Progress*, 30, 1457–1468.
- Young, J. D. (2014). INCA: A computational platform for isotopically non-stationary metabolic flux analysis. *Bioinformatics*, 30, 1333–1335.
- Young, J. D., Walther, J. L., Antoniewicz, M. R., Yoo, H., & Stephanopoulos, G. (2008). An elementary metabolite unit (EMU) based method of isotopically nonstationary flux analysis. *Biotechnology and Bioengineering*, 99, 686–699.
- Zhang, F., Sun, X., Yi, X., & Zhang, Y. (2006). Metabolic characteristics of recombinant Chinese hamster ovary cells expressing glutamine synthetase in presence and absence of glutamine. *Cytotechnology*, 51, 21–28.
- Zhang, J., Fan, J., Venneti, S., Cross, J. R., Takagi, T., Bhinder, B., Djaballah, H., Kanai, M., Cheng, E. H., Judkins, A. R., Pawel, B., Baggs, J., Cherry, S., Rabinowitz, J. D., & Thompson, C. B. (2014). Asparagine plays a critical role in regulating cellular adaptation to glutamine depletion. *Molecular Cell*, 56, 205–218.
- Zhang, L., Zhang, W., Wang, C., Liu, J., Deng, X., Liu, X., Fan, L., & Tan, W. (2016). Responses of CHO-DHFR cells to ratio of asparagine to glutamine in feed media: Cell growth, antibody production, metabolic waste, glutamate, and energy metabolism. *Bioresources and Bioprocessing*, 3, 1–12.
- Zupke, C., Sinskey, A. J., & Stephanopoulos, G. (1995). Intracellular flux analysis applied to the effect of dissolved oxygen on hybridomas. *Applied Microbiology and Biotechnology*, 44, 27–36.

## SUPPORTING INFORMATION

Additional supporting information may be found in the online version of the article at the publisher's website.

**How to cite this article:** Kirsch, B. J., Bennun, S. V., Mendez, A., Johnson, A. S., Wang, H., Qiu, H., Li, N., Lawrence, S. M., Bak, H., & Betenbaugh, M. J. (2022). Metabolic analysis of the asparagine and glutamine dynamics in an industrial Chinese hamster ovary fed-batch process. *Biotechnology and Bioengineering*, 119, 807–819.  
<https://doi.org/10.1002/bit.27993>